



## Study on the Vertical Wall Heat Transfer by Numerical Simulation of Non-Newtonian (Herschel-Bulkley Model) Nanofluid and Changes

Samira Hashemi<sup>1</sup>, Hossein Shokouhmand<sup>2</sup>

<sup>1</sup>Master of Science, Department of Technical & Engineering, West Tehran Branch-Islamic Azad University, IRAN

<sup>2</sup>Professor, School of Mechanical Engineering, University of Tehran, IRAN

Received 23 Jun 2017,  
Revised 05 Jan 2018,  
Accepted 15 Jan 2018

### Keywords

- ✓ Nanofluid
- ✓ Herschel Bulkley,
- ✓ non-Newtonian,
- ✓ Convection,
- ✓ Vertical plate,
- ✓ Numerical simulation.

[Samira.hashemi.2011@gmail.com](mailto:Samira.hashemi.2011@gmail.com)

### Abstract

As plate heat exchangers have numerous applications and there is a lot of heat exchange between solid surfaces and fluids in different industries, the investigation of the heat exchange of fluids with a constant wall heat flux boundary condition, can change an engineer's view in designing heat exchangers including plate heat exchangers. This research deals with numerical investigation of the heat exchange of a nanofluid (with a Non-Newtonian base fluid which has the rheological behavior of Herschel-Bulkley model). As the application of nanofluids especially those with a Non-Newtonian base fluid (such as many lubricating oils whose cooling role in different machinery has been regarded in recent decades) in the matter of heat exchange has not yet completely been recognized, thus, we preferred to use solid nanoparticles in the cooling process of the fluids so that with a growth in the thermal conductivity factor, the heat exchange rate from the fluid to the surface can be increased. In the recent years the use of nanofluids for increasing the heat exchange between fluids and solid surfaces of heat exchangers has become prevalent, so that nowadays in most heat exchange equipment, for a longer durability of components and enhancing the heat exchange rate, different types of nanofluids are utilized due to their high heat exchange factor. In investigating the heat exchange of nanofluids with a Newtonian base fluid (such as water) or Non-Newtonian base fluid (such as different types of industrial oils) two different opinions exist, the assumption of single phase (fluid with solid nanoparticles) and the second is separation of fluid and nanoparticles as liquid and solid phases. Though with the correct determination of equivalent values for density, Viscosity, specific heat capacity and thermal conductivity for the single-phase status, we can obtain precise results and there would be no need for a complicated and lengthy two-phase solution. In most papers, the single-phase assumption is considered.

### 1. Introduction

The topic of heat exchange in nanofluids is a very fascinating topic in the world of science and engineering. The term nanofluids introduced by Choi which represents a liquid suspension containing infinitesimal particles (diameter of less than 50nm). Empirical studies have shown that even in very small volume fractions of nanofluids (less than 5%), the heat conductivity of the base fluid can increase as much as 10%-50%. The growth of heat conductivity besides the thermal emission of particles and the turbulence induced by their movement causes a considerable enhancement in the heat transfer coefficient which itself leads to the nanofluid creating a more appropriate environment for heat transfer in applications such as cooling of advanced nuclear systems and cylindrical heat pipes. Previous studies in the field of heat transfer and viscosity of nanofluids have been executed [1-4].

These studies have details of preparing nanofluids, theoretical and experimental studies of viscosity, conduction of nanofluids and the movement and transfer of nanofluids. A criteria study [5], has been on the conduction of nanofluids. In this paper the empirical data of heat transfer gathered from 30 world organizations have been analyzed and 10% compatibility between them is observed. This research concludes that the conduction of nanofluids increases with the density of particles and also relative to their dimensions, which complies with the classic theory of Maxwell which anticipated that the effective heat ratio ( $k/k_f$ ) is dependent upon the solid

volume fraction of the nanofluid  $f$  and relative heat ratio  $k_p/k_f$ . This functional dependence is valid for  $\Phi \ll 1$  and  $k_p/k_f < 10$ . Another factor of the base fluid which is affected by nanofluids is its viscosity. It has been monitored that the viscosity of nanofluids rises with the rise in the solid volume fraction of the nanofluid. Nonetheless unlike the heat conduction which leads to temperature increase, the viscosity of nanofluids barely changes in temperature fluctuations of 25-89 degrees Celsius. Numerous ideas have been expressed to depict the identity of additional heat transfer in nanofluids. Pak and Cho describe the growth in the heat transfer of nanofluids as a result of emission of particles. Khan and Lee suggested that the increase in the heat transfer of nanofluids is due to the turbulence induced by the movement of nanoparticles. After experiments on water and glycerin based nanofluids, Ahouja concluded that the increase in heat transfer is because of the spinning of nanoparticles. Though after meticulous evaluations, Bounjiormo deduces that the high heat transfer cannot be the result of heat emission, rise of turbulence or the spinning particles. He explains that the analytical model for the movements in nanofluids must be considered in Brownian and Thermophoresis distribution and that the excessive heat transfer is because of the considerable decline in the fluids viscosity due to the large temperature changes in the boundary layers. Research in the field of convective heat transfer has been permanently advancing in the past ten years. Nonetheless the analytical studies on convective heat transfer in nanofluids are much less, compared to studies in forced heat transfer of nanofluids.

Khanfar et al., [6] analyzed the natural two dimensional convection of nanofluids in a crate and understood that for the Grashof number given, the heat transfer rate increases with the increasing solid volume fraction of nanoparticles. In previous work [7], Tou & Zhang introduced a new factor for the depiction of convective instability and characteristics of heat transfer in base fluids. Tezo considered the thermal instability in natural convection and concluded that the additional turbulence due to the nanoparticles causes greater heat transfer coefficient in comparison to the effect of added thermal conductivity. In contrast to the observations, Pruta et al., [8] that the heat transfer coefficient reduces with the solid volume fraction in nanofluids (and does not increase). The difference between the research results of [6-9] may be because of their assumptions in developing their analytical models. In the most recent paper, Abu-Neda et al., [9] studied the effect of varied heat conduction and viscosity on heat transfer on the nanofluid Water-Aluminum Oxide in a locked chamber. They understood that in low Rayleigh numbers, the Nusselt number grows slightly with the increased solid volume fraction of the nanofluid, but in high Rayleigh numbers, that effect is contrariwise. This short research clearly shows that there is still to be a definite conclusion on the role of nanoparticles in raising the natural convective movement. In the past three years, very few articles have worked on the fundamental issues in the external convective flows of nanofluids. In [10] extended the classic natural convection of a fluid from a constant-temperature vertical plane to the flows of nanofluids. They utilized the model of Bounjiormo and considered the Brownian distribution just as Thermophoresis, in writing the transfer equations. Their similar analyze defined four dominant parameters on the transfer process,  $Le$  as the Lewis number,  $Nr$  as the Buoyancy rate,  $Nb$  as the Brownian movement rate,  $Nt$  as the Thermophoresis rate. For constant amounts  $osPr=10$  and  $Le=10$ , the numerical results indicate a reduced Nusselt number, decreases with the increase in each of the parameters  $Nr$ ,  $Nb$ ,  $Nt$ . The Bounjiormo model was used by Khan and Pope for studying the boundary layer flow flowing over a tensile sheet and the model was also utilized by Khan and Aziz for investigating the boundary layer of a nanofluid flowing over a vertical surface with constant heat flux. Other papers to mention on the forced and free convection of nanofluids on horizontal and vertical surfaces [11]. Investigating the flow on a vertical plane with an unstable regime was implemented in [12] with a Non-Newtonian fluid with the power-law model. They concluded that the stability factor in Non-Newtonian fluids have a large effect on the heat exchange. The latest research on the field of heat transfer in Non-Newtonian fluids on a horizontal plane was by [13] which they examined the numeric and analytics of the flows free movement of a Non-Newtonian fluid and they showed that the thermal boundary layer of a Non-Newtonian fluid (with different  $n$ s) for an extended amount of the number in the parenthesis, does not change considerably. Furthermore they added that the maximum velocity of a Non-Newtonian fluid in the hydrodynamic boundary layer is strongly dependent to  $n$  (the stability factor a Non-Newtonian fluid) and with the increase of  $n$  the maximum velocity of the fluid also rises.

## 2. Research Method

In the recent years the flow and heat exchange behavior of Non-Newtonian fluids specifically the fluids of Herschel-Bulkley model have been under scrutiny because of their huge application in different industries such as, food industry, polymer melts, pharmaceutical industry, biotechnology industries and manufacturing of pulp, natural and artificial rubber solutions. The Herschel-Bulkley fluids are the group of Non-Newtonian fluids which have a non-linear relation between tension and strain.

$$\tau = \mu\gamma^n + \tau_y \quad \tau \geq \tau_y \quad (1)$$

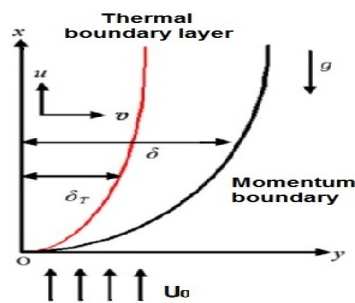
$$\gamma = 0 \quad \tau < \tau_y \quad (2)$$

In the equations (1) and (2),  $n$  (the power-law characteristic) and  $\tau_y$  (the yielding tension) are the rheologic properties of the fluid. In this research the Propellant Dough(35/45) as a Herschel-Bulkley fluid with the thermophysical characteristics mentioned in the table below was selected as the base fluid for the study.

**Table1:** The Thermophysical characteristics of Propellant Dough(35/45) and Nanoparticles [14]

Parameters Material	Consistency (Nsm <sup>-2</sup> )	Thermal conductivity (Wm <sup>-1</sup> K <sup>-1</sup> )	Temperature- shift factor for the viscosity (K <sup>-1</sup> )	Power-Law Index (n)
Propellant Dough(35/45)	17900	0.34	0.0437	0.440
Propellant Dough(35/45)	4330	0.34	0.0437	0.466
Propellant Dough(35/45)	1270	0.34	0.0437	0.533
Al <sub>2</sub> O <sub>3</sub>	-	40	0.85*10 <sup>-5</sup>	-
Parameters Material	Temperature (K)	Density (kgm <sup>-3</sup> )	Specific heat capacity (Jkg <sup>-1</sup> K <sup>-1</sup> )	Yeild stress (kPa)
Propellant Dough(35/45)	293.15	840	1000	39.0
Propellant Dough(35/45)	308.15	840	1000	47.5
Propellant Dough(35/45)	323.15	840	1000	50.0
Al <sub>2</sub> O <sub>3</sub>	-	3970	765	-

From the table below, the Reynolds number and the temperature difference between the vertical separation wall and the adjacent fluid in 20°C was extracted [14].



Reynolds number	temperature (°C) difference
1.5*10 <sup>-4</sup>	9.1
4.5*10 <sup>-4</sup>	16.9
1.3*10 <sup>-3</sup>	24.0

**Figure 1:** A schematic diagram of the physical model under investigation

The Richardson and Grashov numbers are calculated from the equations below:

$$Ri = \frac{Gr}{Re^2} \quad (3)$$

$$Gr = \frac{g(\beta)_f(T_w - T_\infty)L^3}{\nu^2} \quad (4)$$

From the equations above we can conclude that for this problem,  $\frac{Gr}{Re^2} \ll 1$  and therefore the forced movements can be ignored and regarding the Reynolds number assumed ( $Re \approx 10^{-3}$ ) and the type of fluid as a base fluid (fluid with high viscosity) and the creeping flow theory which is prevailing over this case, we can consider the movements as natural movements compare the results with the results of research done in field of natural movement.

### 3. The Equations Dominating the Problem

For describing the flow of a slimy and incompressible fluid, the laws of mass conservation, momentum and energy conservation are used. For the flow of a nanofluid, the equation of mass conservation (5), momentum conservation (6) and energy conservation (7) are depicted below:

$$\frac{\partial u}{\partial x} + \frac{\partial v}{\partial y} = 0 \quad (5)$$

$$\left(u \frac{\partial u}{\partial x} + v \frac{\partial u}{\partial y}\right) = (\vartheta_{nf}) \left(\frac{\partial^2 u}{\partial x^2} + \frac{\partial^2 u}{\partial y^2}\right) + (\beta)_{nf} g(T - T_{\infty}) \quad (6)$$

$$u \frac{\partial T}{\partial x} + v \frac{\partial T}{\partial y} = \alpha_{nf} \left(\frac{\partial^2 T}{\partial y^2}\right) \quad (7)$$

All the equations are written for a uniform status. Density, diffusion, heat capacity and thermal expansion coefficient of the nanofluid are in equations (8) to (11) respectively:

$$\rho_{nf} = (1 - \phi)\rho_f + \phi\rho_p \quad (8)$$

$$\alpha_{nf} = k_{nf}/(\rho c_p)_{nf} \quad (9)$$

$$(\rho c_p)_{nf} = (1 - \phi)(\rho c_p)_f + \phi(\rho c_p)_p \quad (10)$$

$$(\rho\beta)_{nf} = (1 - \phi)(\rho\beta)_f + \phi(\rho\beta)_p \quad (11)$$

For consistency of the nanofluid, three equations have been expressed in which the first equation (12) is the Brinkman formula and the other two (13) and (14) are empirical formulas.

$$\mu_{nf} = \mu_f / (1 - \phi)^{\frac{2}{5}} \quad (12)$$

$$\mu_{nf} = \mu_f (1 + 39.11\phi + 533.9\phi^2) \quad (13)$$

$$\mu_{nf} = \mu_f (1 + 7.3\phi + 123\phi^2) \quad (14)$$

For the thermal conductivity of the nanofluid, 2 equations are stated. The first one (15) is the Maxwell formula and the next one (16) is an empirical formula.

$$k_{nf} = k_f \left[ \frac{(k_p + 2k_f) - 2\phi(k_f - k_p)}{(k_p + 2k_f) + \phi(k_f - k_p)} \right] \quad (15)$$

$$k_{nf} = k_f (1 + 7.47\phi) \quad (16)$$

The boundary conditions for this case are:

$$y = 0, \quad u = v = 0, \quad -k \frac{\partial T}{\partial y} = q_w''$$

$$y \rightarrow \infty, \quad u \rightarrow U_{\infty}, \quad T \rightarrow T_{\infty} \quad (17)$$

Defining the dimensionless variables:

$$X = \frac{x}{L}, \quad Y = \frac{y}{L} Re^{1/2}, \quad U = \frac{u}{U_{\infty}}, \quad V = \frac{v}{U_{\infty}} Re^{1/2}, \quad \eta = \frac{y}{x} Ra_x^{1/4}, \quad -k \frac{\partial T}{\partial y} = q_w''$$

$$P = \frac{\bar{p}L^2}{\rho_{nf}\alpha_f^2}, \quad Ra = \frac{g\beta_f L^3 \Delta T}{\nu_f \alpha_f}, \quad Re = \frac{U_{\infty} L}{\vartheta}, \quad Gr = \frac{g\beta_f L^3 \Delta T}{\vartheta^2}, \quad Pr = \frac{\nu_f}{\alpha_f}, \quad Br = \frac{\mu_f u^2}{k_f(T_w - T_{\infty})} \quad (18)$$

Mass conservation equations, Momentum conservation and Energy conservation are rewritten dimension less in the form below:

$$\frac{\partial U}{\partial X} + \frac{\partial V}{\partial Y} = 0 \quad (19)$$

$$U \frac{\partial U}{\partial X} + V \frac{\partial U}{\partial Y} = \left( \frac{\partial^2 U}{\partial Y^2} \right) + \frac{Gr}{Re^2} \theta \quad (20)$$

$$U \frac{\partial \theta}{\partial X} + V \frac{\partial \theta}{\partial Y} = \frac{1}{Pr} \left( \frac{\partial^2 \theta}{\partial Y^2} \right) \quad (21)$$

The boundary conditions are rewritten as dimensionless:

$$Y = 0, \quad U = V = 0, \quad \theta' = -1$$

$$Y \rightarrow \infty, \quad U \rightarrow 1, \quad \theta \rightarrow 0 \quad (22)$$

The local Nusselt number on the surface of the heat source is driven from the equation below:

$$Nu_s = \frac{hL}{k_f} \quad (23)$$

The local thermal exchange coefficient (h) is defined as below:

$$h = \frac{q''}{T_w - T_\infty} \quad (24)$$

The average thermal exchange coefficient ( $\bar{h}$ ) is defined as below:

$$\bar{h} = \frac{1}{L} \int_0^L h \, dx \quad (25)$$

With making the parameters dimensionless and applying the equations (23), (24) can be rewritten as seen below:

$$Nu_w(X) = \frac{1}{\theta_w(X)} \quad (26)$$

The surface friction coefficient and the shear stress on the wall can be calculated from the equations below:

$$C_f = \frac{\tau_w}{0.5\rho v^2} \quad (27)$$

$$\tau_w = \mu \frac{\partial u}{\partial y} \quad (28)$$

The local and average Nusselt according to Reynolds and Rayleigh number in a laminar flow with a constant wall heat flux boundary condition can be calculated from the equations below:

$$Nu = 0.616(Ra)^{1/5} \quad (\text{for high Prandtl numbers}) \quad (29)$$

$$Nu_x = 0.453(Re_x)^{0.5} (Pr)^{1/3} \quad (0 < Re_L < 5 \times 10^5, \quad Pr > 0.6) \quad (30)$$

## 4. Results

### 4.1. Investigating the Nusselt number in different types of volume fractions of nanoparticles

The Nusselt is considered on the vertical wall. From the diagrams it is obvious that when the nanoparticles are added, the Nusselt number and consequently the heat exchange increase which this increase is around 4% in volume increase from the maximum limit of volume. Figure 2 illustrates the Part of the Nusselt number profile in the length of the vertical wall for types of volume fraction of nanoparticles (nanofluids Al<sub>2</sub>O<sub>3</sub>/Propellant Dough(35/45)) – the fluid temperature of 20°C and temperature difference of fluid and wall 27.8°C and the Reynolds number equal to 1.3\*10<sup>-3</sup> and n=0.440. Also, the Average Nusselt Number Profile in the length of the vertical wall for types of volume fraction of nanoparticles (nanofluids Al<sub>2</sub>O<sub>3</sub>/Propellant Dough (35/45)) is shown in figure 3. The fluid temperature of 20°C and temperature difference of fluid and wall 27.8°C and the Reynolds number equal to 1.3\*10<sup>-3</sup> and n=0.440.

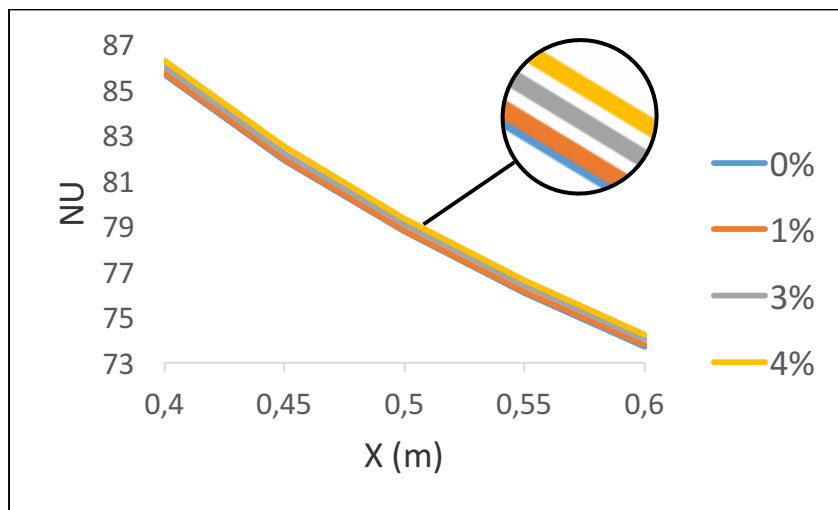


**Figure 2:** Part of the Nusselt number profile in the length of the vertical wall for types of volume fraction of nanoparticles (nanofluids  $\text{Al}_2\text{O}_3/\text{Propellant Dough}$  (35/45))

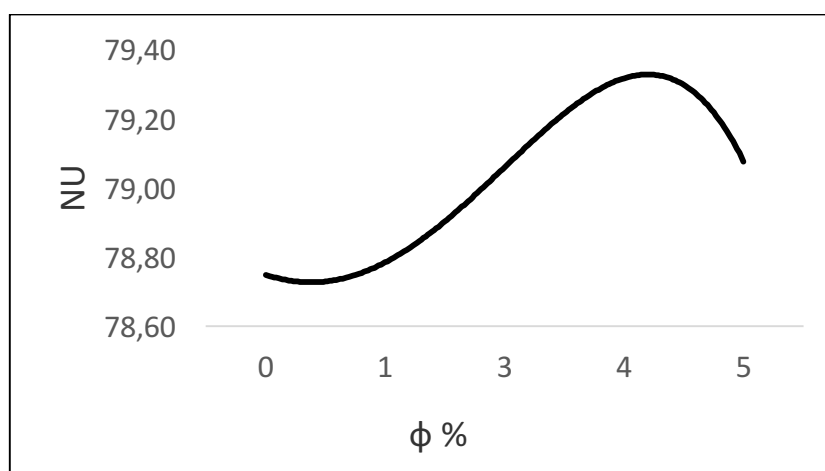


**Figure 3:** The Average Nusselt Number Profile in the length of the vertical wall for types of volume fraction of nanoparticles (nanofluids  $\text{Al}_2\text{O}_3/\text{Propellant Dough}$  (35/45))

According to the tables and diagrams below, both the amounts of thermal conductivity ( $k$ ) and convection heat exchange coefficient ( $h$ ) increase as the volume fraction of nanoparticles increase. Up to 4% volume fraction the increase in the convection heat exchange coefficient is higher than thermal conductivity, which causes the Nusselt number to increase. In higher volume fractions the effect on (increasing) the thermal conductivity is higher than convection heat exchange coefficient which leads to the decrease of the Nusselt number.

**Table 2:** Comparing the ratio of  $h/k$  for types of volume fraction of nanoparticles (nanofluids  $\text{Al}_2\text{O}_3/\text{Propellant Dough}$  (35/45))

Volume fraction	Convection heat exchange coefficient	Thermal conductivity	Ratio of $h/k$
%0	492	0.34	1445.6
%1	506	0.35	1447.1
%3	536	0.37	1449.6
%4	551	0.38	1449.8
%5	564	0.39	1446.6

Figure r shows the Profile of Heat Exchange Coefficient in the length of the vertical wall for types of volume fraction of nanoparticles (nanofluids  $\text{Al}_2\text{O}_3/\text{Propellant Dough}$  (35/45)). The fluid temperature of  $20^\circ\text{C}$  and temperature difference of fluid and wall  $27.8^\circ\text{C}$ ,  $24^\circ\text{C}$  and the Reynolds number equal to  $1.3 \cdot 10^{-3}$  and  $n=0.440$ . Figure 5 shows the Profile of Thermal Conductivity in the length of the vertical wall for types of volume fraction of nanoparticles (nanofluids  $\text{Al}_2\text{O}_3/\text{Propellant Dough}$  (35/45)). The fluid temperature of  $20^\circ\text{C}$  and temperature difference of fluid and wall  $27.8^\circ\text{C}$  and  $24^\circ\text{C}$ , the Reynolds number equal to  $1.3 \cdot 10^{-3}$  and  $n=0.440$ .

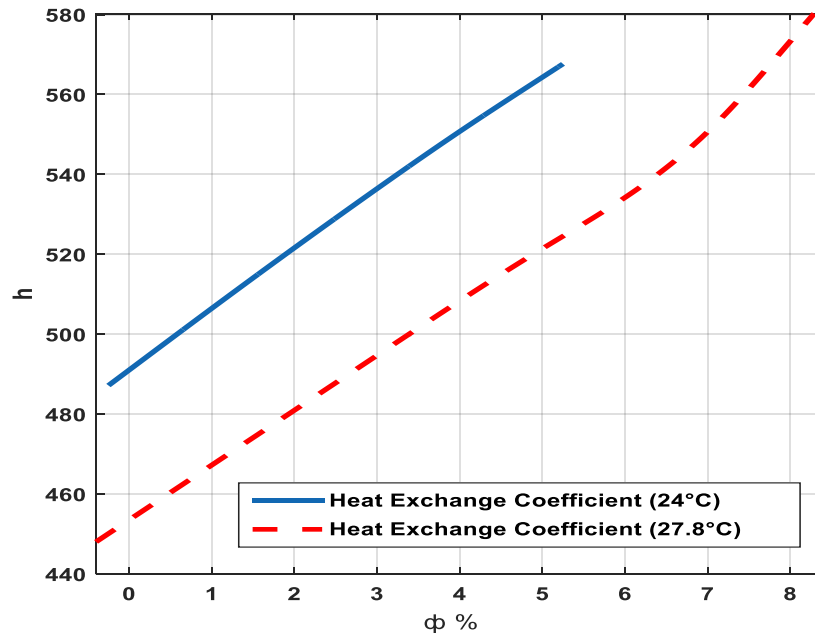


**Figure 4:** The Profile of Heat Exchange Coefficient in the length of the vertical wall for types of volume fraction of nanoparticles (nanofluids  $\text{Al}_2\text{O}_3$ /Propellant Dough (35/45))

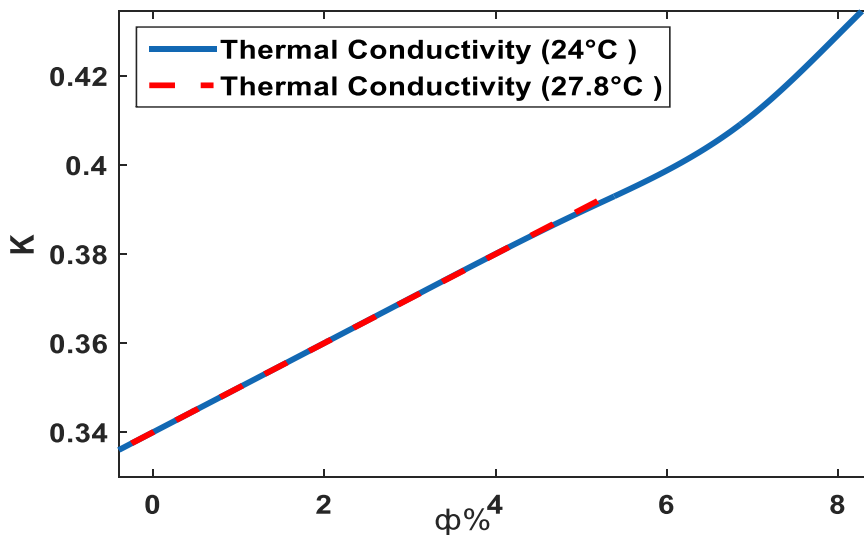


**Figure 5:** The Profile of Thermal Conductivity in the length of the vertical wall for types of volume fraction of nanoparticles (nanofluids  $\text{Al}_2\text{O}_3$ /Propellant Dough(35/45))

#### 4.2. Investigating surface friction coefficient in the volume fraction of nanoparticles

The value of friction coefficient is investigated on vertical plane. According to the following diagrams it is obvious that it is reduced along the wall and when nanoparticles are added, surface friction coefficient decreases. The fluid temperature of  $20^\circ\text{C}$  and temperature difference of fluid and wall  $27.8^\circ\text{C}$  and the Reynolds number equal to  $1.3 \times 10^{-3}$  and  $n=0.440$ .

As shown in the figure 7, the pressure is decreased with an increase in the length of the wall, and due to direct impact of pressure on surface friction coefficient, this parameter is also decreased along the wall.

With the increase of volume fraction of nanoparticles, density and dynamic viscosity increase. According to equation (27) and (28), density has a reverse impact on friction coefficient and direct impact on dynamic viscosity. Up to a volume fraction of 4 percent the effect of density changes is more than the effect of dynamic viscosity changes.

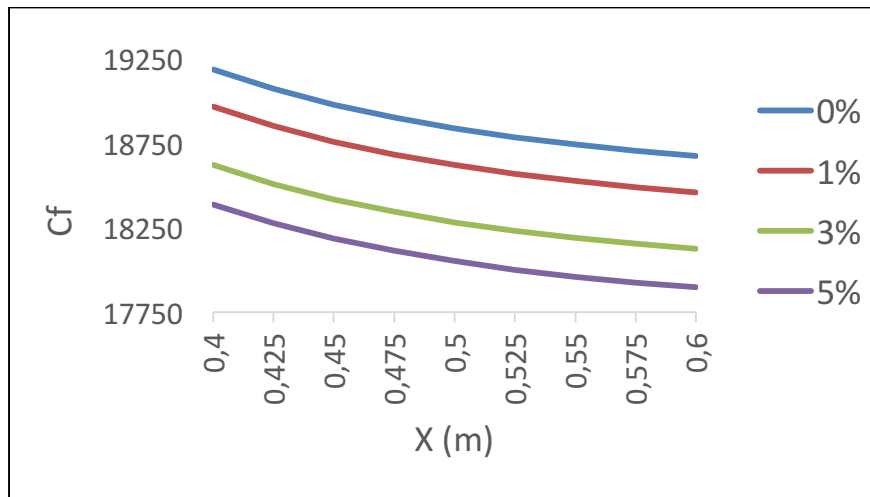


**Figure 6:** A part of surface friction coefficient profile in the length of the vertical wall for types of volume fraction of nanoparticles (nanofluids  $Al_2O_3$ /Propellant Dough(35/45)).

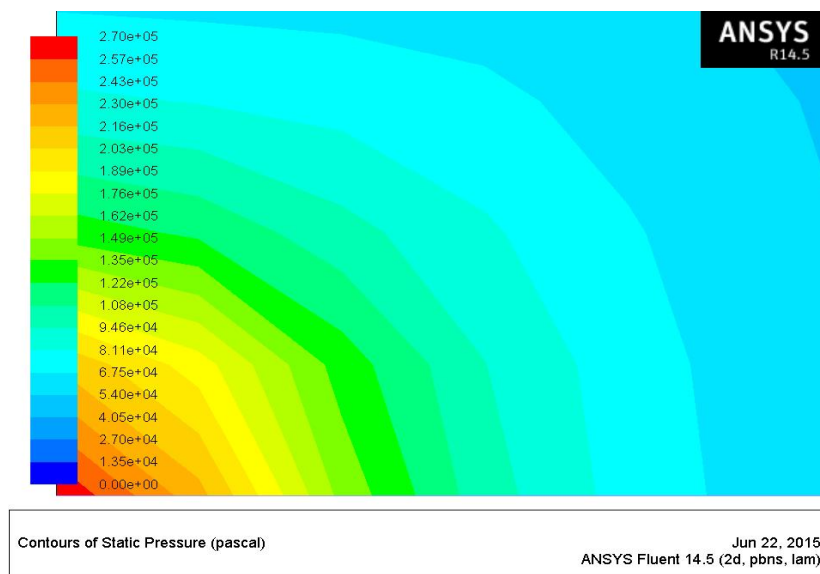


**Figure 7:** Pressure contour along the flow path

#### 4.3. Investigation of temperature and velocity in boundary layer in the volume fraction of nanoparticles

As is shown in figure 8, the increase of volume fraction of nanoparticles does not have any considerable effect on dimensionless velocity in boundary layer but with the increase of volume fraction of nanoparticles, the dimensionless temperature on the wall decreases in the state of constant heat flux on the vertical wall and according to equation (26), the Nusselt number on the wall increases and such result is evident in local and average Nusselt charts for different volume fractions.

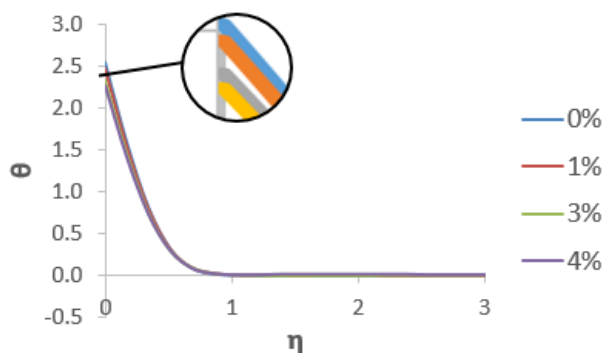


**Figure 8:** Dimensionless temperature changes profile for volume fraction of nanoparticles (Nanofluids  $Al_2O_3$ /Propellant Dough(35/45))

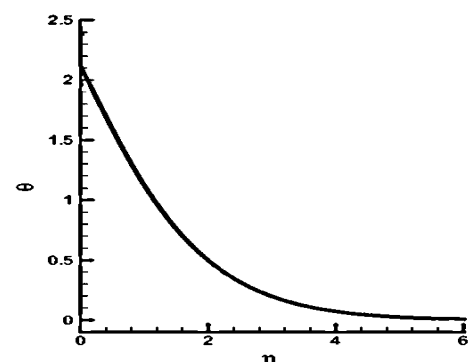


**Figure 9:** Dimensionless temperature profile with boundary condition of constant heat flux on the vertical wall for nanofluid [15]

As is shown in above diagrams, the results obtained in this research are in agreement with the results achieved by Aziz and Khan [15].

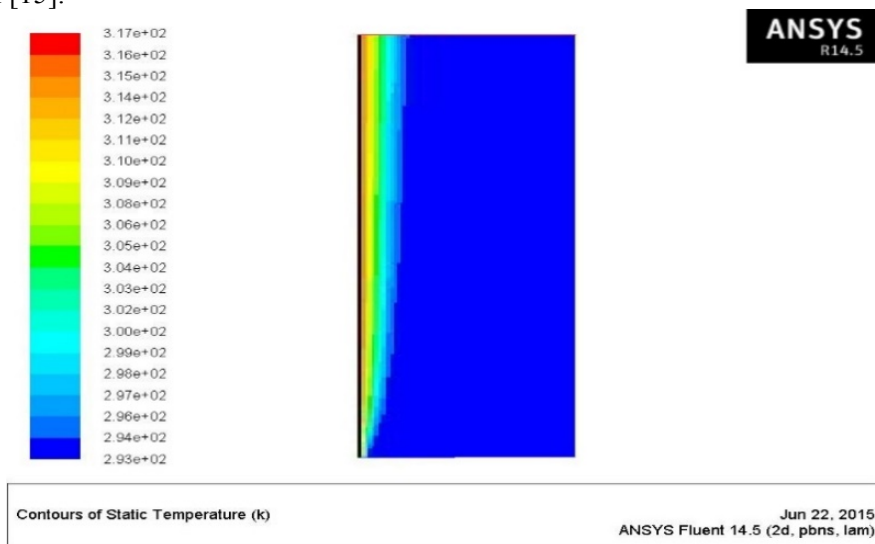


Figure 10: Contour of boundary layer formed on vertical wall

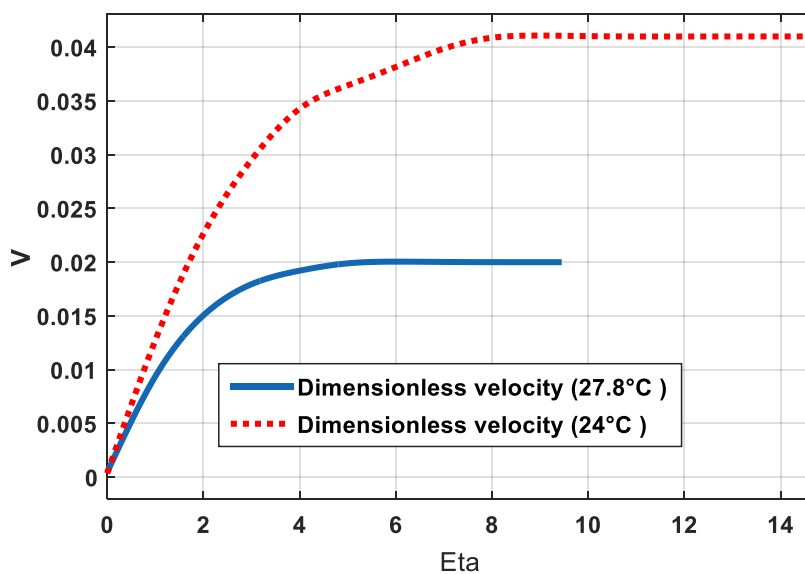


Figure 11: Dimensionless velocity changes profile for volume fraction of nanoparticles (Nanofluids  $Al_2O_3$ /Propellant Dough(35/45)) – fluid temperature is  $20^\circ C$  and temperature difference between fluid and wall is  $27.8^\circ C$  and  $24^\circ C$  and Reynolds number is  $1.3 \times 10^{-3}$  and  $n=0.440$

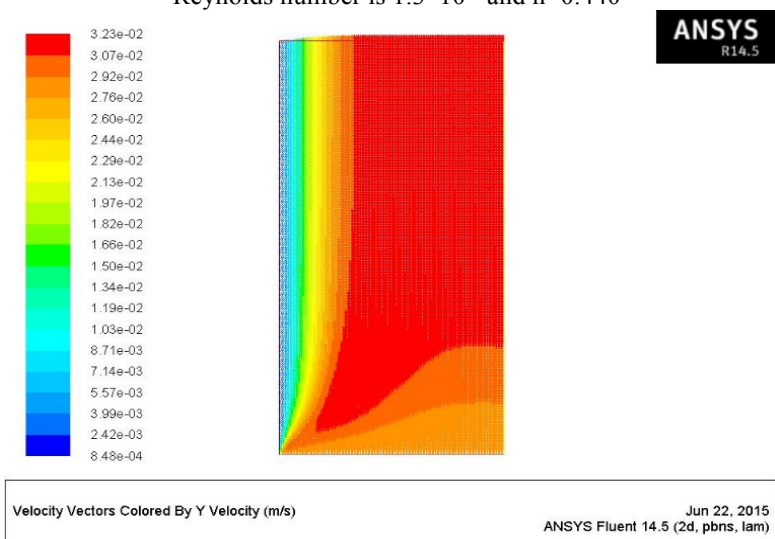
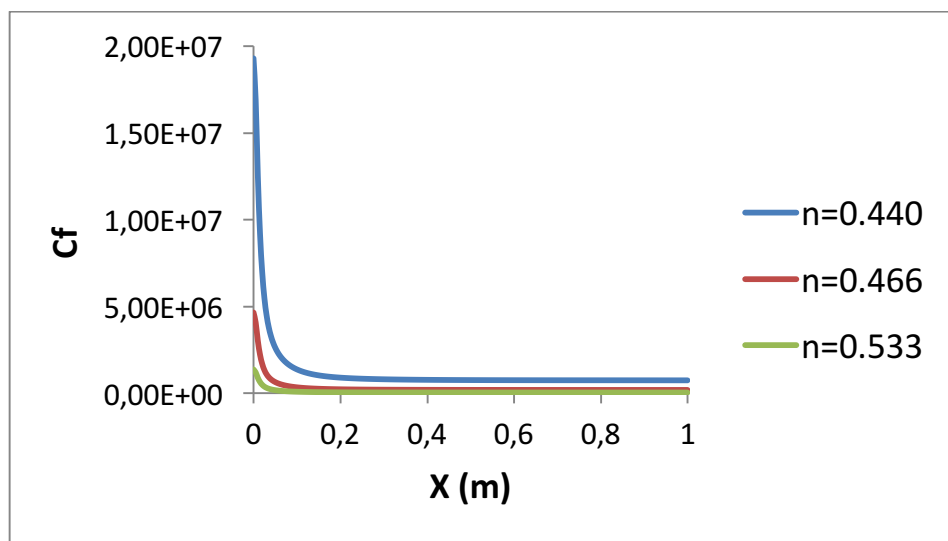


Figure 12: Contour of hydrodynamic boundary layer formed on vertical wall

4.4. The effect of rheological properties and yield stress of the base fluid on the Nusselt number, surface friction coefficient and velocity and temperature in boundary layer

The value of Nusselt number and friction coefficient on the vertical wall is investigated. According to the following diagrams it is obvious that when  $n$  (Rheological properties of the base fluid) and so yield stress of the base fluid is increased, surface friction coefficient decreases. It must be noted that according to these diagrams, increase of  $n$  and yield stress of the base fluid does not have a considerable effect on the Nusselt number, temperature and velocity in the boundary layer.



**Figure 13:** Surface friction coefficient profile along the vertical wall for the volume fraction of 4% of nanoparticles (Nanofluids  $\text{Al}_2\text{O}_3/\text{Propellant Dough}(35/45)$ ) – Reynolds number is  $4.5 \times 10^{-4}$

According to the table of rheological properties of liquid propellant (35/45), increase of  $n$  reduces dynamic viscosity and based on equation (27) and (28), dynamic viscosity has a direct impact on friction coefficient and so by increase of  $n$  surface friction coefficient is decreased.

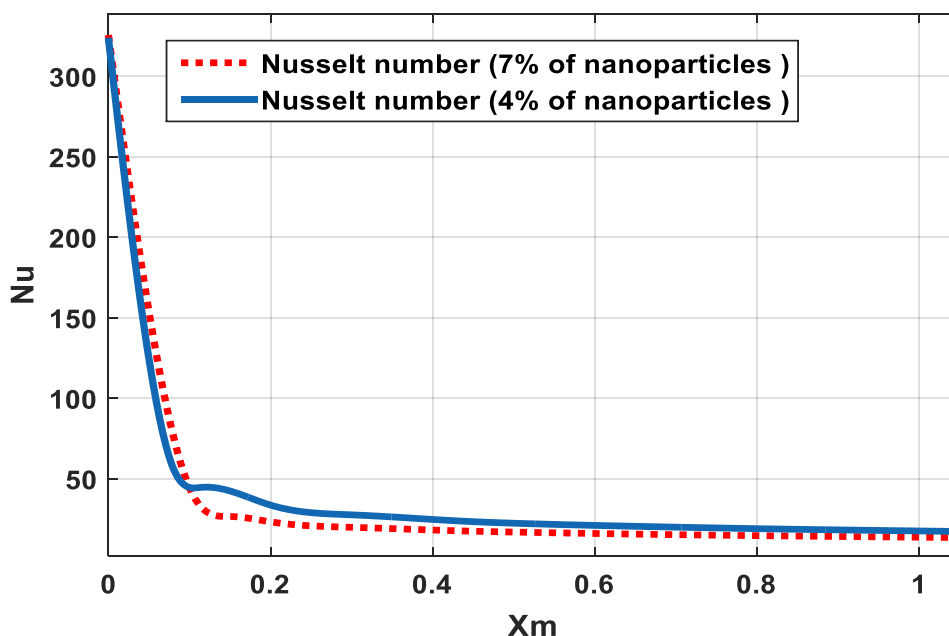


**Figure 14:** Nusselt number profile along the vertical wall for the volume fraction of 7% and 4% of nanoparticles (Nanofluid  $\text{Al}_2\text{O}_3/\text{Propellant Dough}(35/45)$ ) – Reynolds number is  $4.5 \times 10^{-4}$

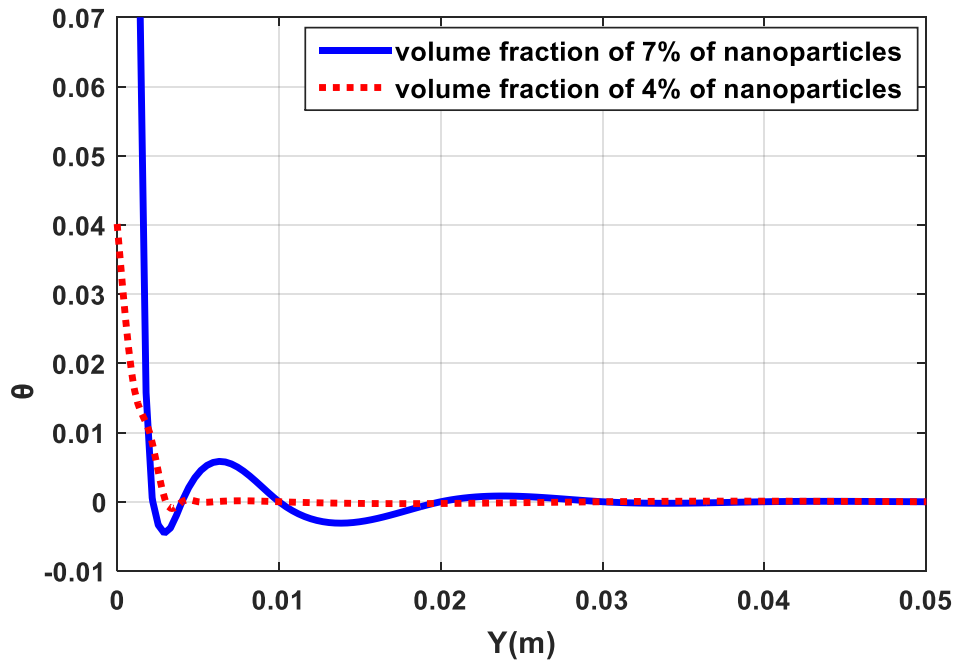


**Figure 15:** Dimensionless temperature profile for the volume fraction of 7% and 4%, of nanoparticles (Nanofluid  $\text{Al}_2\text{O}_3/\text{Propellant Dough}$  (35/45)) - Reynolds number is  $4.5 \times 10^{-4}$

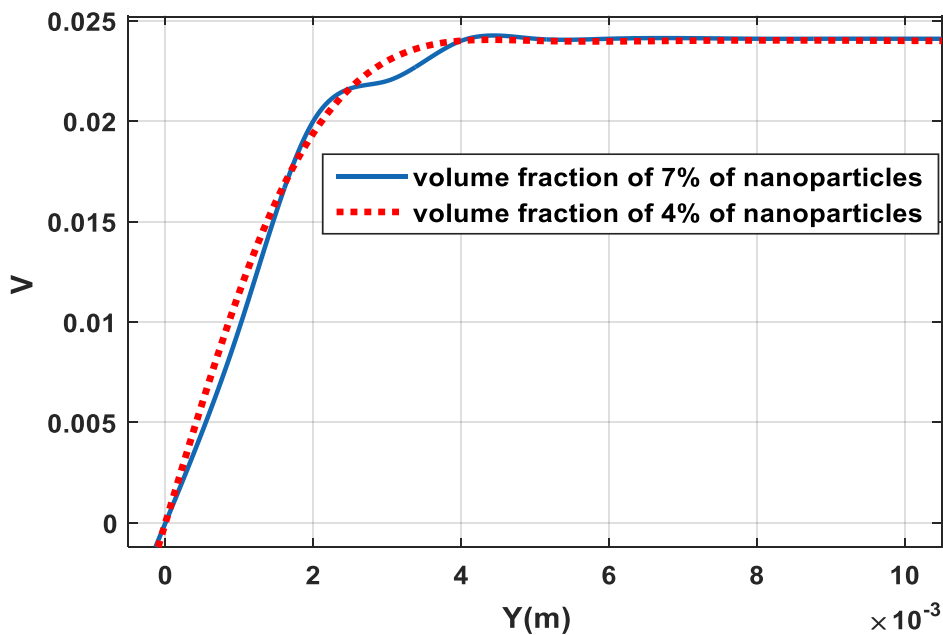


**Figure 16:** Dimensionless velocity profile for the volume fraction of 7% and 4%, of nanoparticles (Nanofluid  $\text{Al}_2\text{O}_3/\text{Propellant Dough}$  (35/45)) - Reynolds number is  $4.5 \times 10^{-4}$

*4.5. The effect of Brinkman number changes on the Nusselt number and surface friction coefficient*

The value of Nusselt number and friction coefficient on the vertical wall is investigated. According to the Figures 17 and 18 which are presenting the nusselt number along the vertical wall based on Brinkman number, it is obvious that when Brinkman number is increased along the wall, Nusselt number and so thermal transfer and surface friction coefficient is increased. The Reynolds number is considered  $1.3 \times 10^{-3}$  and  $n=0.440$  for the volume fraction of 4% of nanoparticles (Nanofluids  $\text{Al}_2\text{O}_3/\text{Propellant Dough}$  (35/45)).

By flow passing along the vertical wall the temperature of wall is increased and according to equation (18), the temperature of wall has a reverse impact on the Brinkman Number. Also from

local and average Nusselt diagrams in different volume fraction it is evident that by moving up along the wall, Nusselt number and surface friction coefficient is decreased. So, it can be concluded that Nusselt number and surface friction coefficient have a direct relation with Brinkman number.

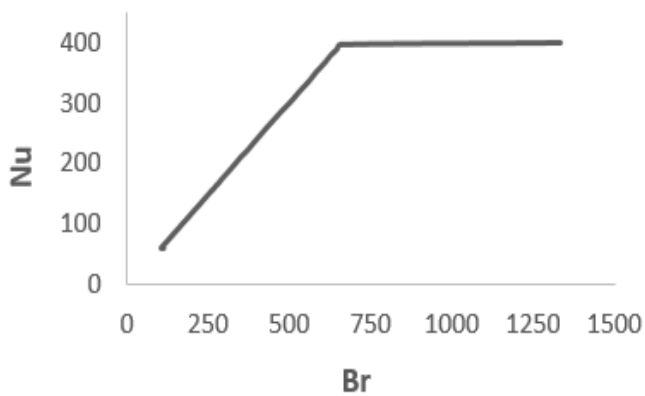


**Figure 17:** Nusselt number along the vertical wall versus to Brinkman number

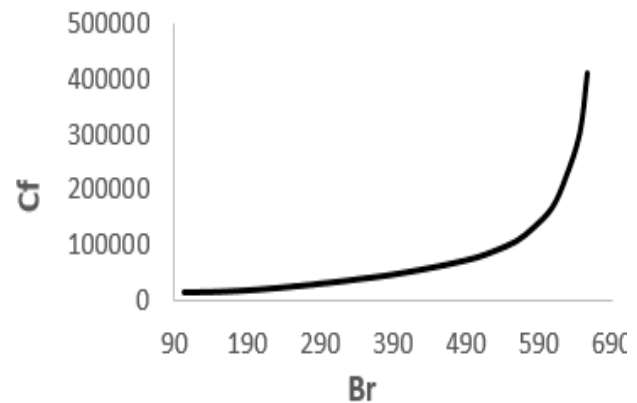


**Figure 18:** Surface friction along the vertical wall versus to Brinkman number

## Discussion and conclusions

In this study, combined convection on a vertical plate with the boundary condition of constant wall heat flux on the wall with non-Newtonian nanofluid of  $\text{Al}_2\text{O}_3/\text{Propellant Dough}$  (35/45) is investigated numerically. The flow is assumed to be laminar, stable, incompressible, viscous and two-dimensional. The effects of volume fraction of nanoparticles and rheological index of base fluid and Brinkman number changes on the wall thermal transfer is studied. The important results obtained from this study are as following:

- 1- The effects of percentage of nanoparticle of Aluminum oxide are investigated on heat transfer on walls.
- 2- Adding nanoparticle of Aluminum oxide to the base fluid increased local and average Nusselt number that this increase has its maximum value at the volume fraction of 7%.
- 3- Adding nanoparticle of Aluminum oxide to the base fluid increased thermal conductivity and thermal transfer coefficient at all volume fractions.
- 4- The value of friction coefficient on the vertical plane decreases along the wall.
- 5- When nanoparticles are added to the base fluid the surface friction coefficient decreases.
- 6- Growth of volume fraction of nanoparticles does not have a considerable effect on velocity in the boundary layer.
- 7- Increase of volume fraction of nanoparticles leads to the decrease of dimensionless temperature on the vertical wall.
- 8- When rheological properties of base fluid and so yield stress of base fluid is increased, the surface friction coefficient is decreased.
- 9- Increase of rheological properties and yield stress of base fluid do not have a considerable effect on Nusselt number, temperature and velocity in the boundary layer.
- 10- When Brinkman number is increase along the wall, Nusselt number and so thermal transfer are also increased.
- 11- Rise of Brinkman number leads to the increase of surface friction coefficient.

## References

1. Tiago Augusto, Moreira Francisco, Júlio do Nascimento, Gherhardt Ribatski, *Experimental Thermal and Fluid Science*, 89(2017) 72-89.
2. M. Hatami, D.D. Ganji, *Case Studies of Thermal Engineering 2* (2014) 14-22.

3. N. Labsi, Y.K. Benkahla, B. Abdelkader, *20th European Symposium on Computer Aided Process Engineering – ESCAPE20*, (2010) Elsevier B.V.
4. A. Aziz, W.A. Khan, *International Journal of Thermal Sciences*, 52 (2012) 83-90
5. K. AbdulHamid, W.H. Azmia, M.F. Nabil, *International Journal of Heat and Mass Transfer*, 118 (2018) 617-627.
6. K. Khanafer, K. Vafai, M. Lightstone, *International Journal of Heat and Mass Transfer*, 46 (19) (2003) 3639-3653.
7. S. K.W. Tou, X. F. Zhang, *International Journal of Heat and Mass Transfer*, 46 (1) (2003) 127-138.
8. N. Pruta, W. Roetzel, S. K. Das, *Heat Mass Transfer*, 39 (2003) 775-784.
9. O. Abuali, A. Falahatpisheh, *Journal of Heat and Mass Transfer*, 46 (1) (2009) 15-23.
10. A. Sh. Kherbeet, H.A. Mohammed, B.H. Salman, Ahmed, E. Hamdi Alawi, A. Omer, M.M. Rashidi, *Experimental Thermal and Fluid Science*, 23 February (2015).
11. Muhammad Noor Afiq Witri Muhammad Yazid, Nor Azwadi CheSidika, Wira Jazair Yahya, *Renewable and Sustainable Energy Reviews*, 80(2017) 914-941.
12. S. M. Aminossadati, B. Ghasemi, *European Journal of Mechanics B/Fluids*, 28 (5) (2009) 630-640.
13. G. C. Bourantas, V.C. Loukopoulos, *International journal of Heat and mass transfer*, 68 (2014) 35-41.
14. E. Mitsoulis, A.A. Abdali, *The Canadian Journal of Chemical Engineering*, 71, (1993).
15. A. Aziz, W.A. Khan, *International Journal of Thermal Sciences*, 50 (2011), 1207-121.

(2018) ; <http://www.jmaterenvirosci.com>